Eur Biophys J (2005) 34: 469–476
DOI 10.1007/s00249-005-0491-y

ARTICLE

**Matthew A. Perugini · Michael D. W. Griffin
Brian J. Smith · Lauren E. Webb · Antony J. Davis
Emanuela Handman · Juliet A. Gerrard**

Insight into the self-association of key enzymes from pathogenic species

Received: 2 December 2004 / Accepted: 12 May 2005 / Published online: 25 June 2005

Abstract Self-association of protein monomers to higher-order oligomers plays an important role in a plethora of biological phenomena. The classical biophysical technique of analytical ultracentrifugation is a key method used to measure protein oligomerisation. Recent advances in sedimentation data analysis have enabled the effects of diffusion to be deconvoluted from sample heterogeneity, permitting the direct identification of oligomeric species in self-associating systems. Two such systems are described and reviewed in this study. First, we examine the enzyme dihydrodipicolinate synthase (DHDPS), which crystallises as a tetramer. Wild-type DHDPS plays a critical role in lysine biosynthesis in microbes and is therefore an important antibiotic target. To confirm the state of association of DHDPS in solution, we employed sedimentation velocity and sedimentation equilibrium studies in an analytical ultracentrifuge to show that DHDPS exists in a slow dimer–tetramer equilibrium with a dissociation constant of 76 nM. Second, we review works describing the hexamerisation of GDP-mannose pyrophosphorylase (GDP-MP), an enzyme that plays a critical role in mannose metabolism in *Leishmania* species. Although the structure of the GDP-MP hexamer has not yet been determined, we describe a three-dimensional model of the hexamer based largely on homology with the uridyltransferase enzyme, Glmu. GDP-MP is a novel drug target for the treatment of leishmaniasis, a devastating parasitic disease that infects more than 12 million people worldwide. Given that both GDP-MP and DHDPS are only active in their oligomeric states, we propose that inhibition of the self-association of critical enzymes in disease is an emerging paradigm for therapeutic intervention.

Keywords Analytical ultracentrifugation · Binding · Bioinformatics · Drug discovery · Enzyme · Leishmania · Protein-protein interactions · Sedimentation · Structural modeling

M. A. Perugini (✉) · L. E. Webb
Department of Biochemistry and Molecular Biology,
Bio21 Molecular Science and Biotechnology Institute,
University of Melbourne, Parkville,
Victoria, 3010, Australia
E-mail: perugini@unimelb.edu.au
Tel.: +61-3-83442355
Fax: +61-3-93481421

M. D. W. Griffin · J. A. Gerrard
School of Biological Sciences,
University of Canterbury,
Christchurch, New Zealand

M. D. W. Griffin
NZ Institute of Crop and Food Research Ltd.,
Private Bag 4704, Christchurch, New Zealand

B. J. Smith
Structural Biology Division,
Walter and Eliza Hall Institute,
Parkville, Australia

A. J. Davis · E. Handman
Infection and Immunity Division,
Walter and Eliza Hall Institute,
Parkville, Australia

Introduction

Protein hetero-association and self-association play essential roles in biology (Marianayagam et al.. 2004). One example of the importance of protein oligomerisation in biological mechanisms is allosteric regulation. This is traditionally illustrated with hemoglobin and oxygen binding (Yonetani et al. 2002) and in the control of critical rate-limiting steps with enzymes such as phosphofructokinase (Fenton et al. 2004). More recently, the modulation of protein function by oligomeric state has emerged as a common theme in the literature. A change in quaternary structure is often associated with a change in function, and transient protein–protein interactions can thus be important biological regulators (Nooren and Thornton 2003). For some enzymes, such as UDP-glucose pyrophosphorylase from barley, the monomer is the active species and the oligomer is

apparently inactive (Martz et al. 2002). With other enzymes, such as HIV-1 protease, the opposite is the case. The requirement for a dimeric structure in HIV-1 protease has been exploited in the design of novel drugs that disrupt the quaternary structure and inactivate the enzyme (Boggetto and Reboud-Ravaux 2002). Similar principles have been applied to the design of inhibitors of *Plasmodium falciparum* triose phosphate isomerase, with a view to disrupting the homodimeric enzyme in order to effect inhibition (Singh et al. 2001).

In this paper, we highlight the potential to make disruption of enzyme self-association a general paradigm for drug design, and illustrate the concept with a discussion of two important drug targets: dihydrodipicolinate synthase (DHDPS) and GDP-mannose pyrophosphorylase (GDP-MP). In addition, we emphasize that analytical ultracentrifugation is an essential tool for analysing protein self-association, and review recent advances that permit detailed analyses of protein–protein interactions in solution.

Dihydrodipicolinate synthase

Given the increasing prevalence of antibiotic resistance, new targets are sought in antibiotic design. One target of antibacterial agents that has yet to be fully exploited is the biosynthesis of the amino acid lysine and its immediate precursor *meso*-diaminopimelate (*meso*-DAP) (Hutton et al. 2003). The lysine biosynthetic pathway in plants and bacteria yields the de novo synthesis of lysine for protein utilisation. More importantly, lysine and *meso*-DAP are vital constituents of the bacterial peptidoglycan cell wall (Hutton et al. 2003). Hence, blockage of lysine (and *meso*-DAP) biosynthesis would inhibit bacterial growth via two mechanisms, and such inhibitors may provide a new class of antibacterial agents. The occurrence of the lysine biosynthetic pathway in microorganisms and plants, but not in mammals, suggests that specific inhibitors of this biosynthetic pathway may display novel antibacterial properties with low mammalian toxicity. Thus, the lysine biosynthetic pathway in general, and the branch point enzyme DHDPS in particular, have become a focus of attention in antibiotic design. Despite this, no potent inhibitor has yet been found for an enzyme in this pathway.

Biochemical and structural analyses demonstrate that *Escherichia. coli* DHDPS forms a tetramer with a large cavity in the centre of the enzyme (Mirwaldt et al. 1995) (Fig. 1). The product of the reaction, lysine, can bind to a specific pocket between the tight dimer–dimer interface, as shown in Fig. 1, and effect negative allosteric feedback regulation. Since both catalytic and regulatory sites are contained within the tight dimer, the reason that *E. coli*

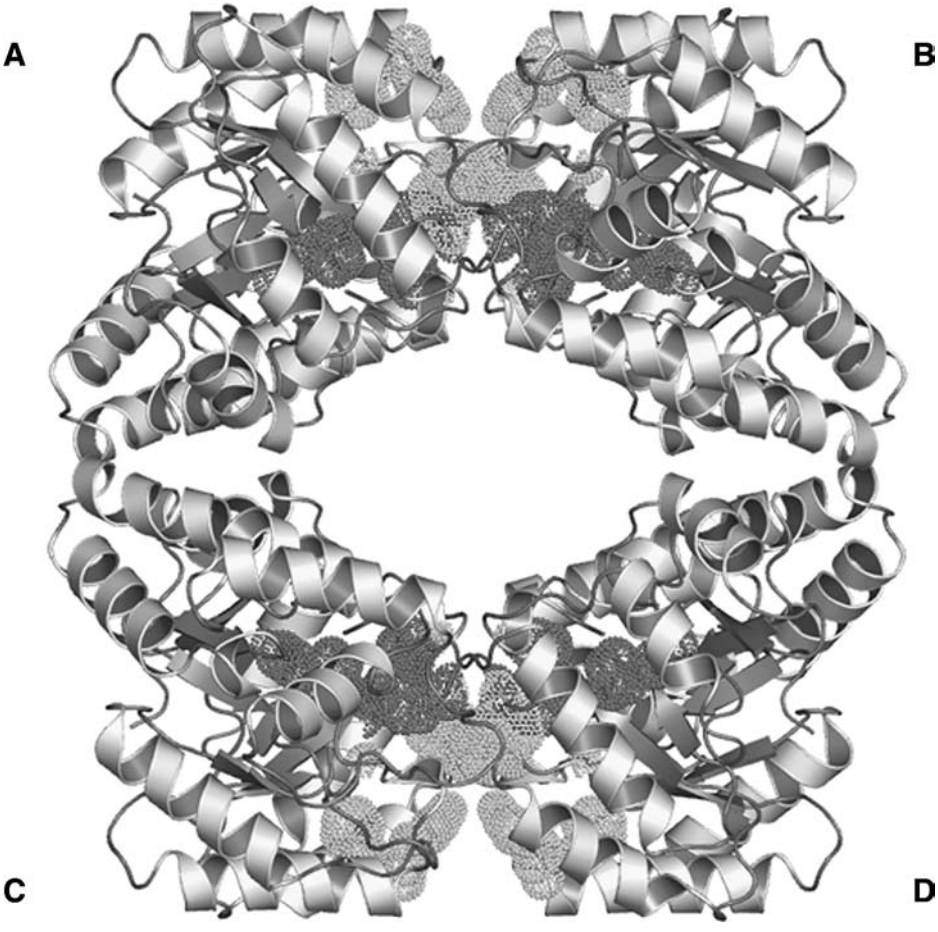

Fig. 1 Tetrameric structure of DHDPS from *E. coli*. Monomers A and B, and monomers C and D associate via an extensive interface to form the tight-dimer. Two dimers associate across less extensive interfaces to produce the tetramer. Essential active site residues are shown in *red*, and lysine-binding residues are shown in *green*. Figure produced using the open source program, PyMol, which is available from http://www.pymol.org

DHDPS adopts the tetrameric form is unclear. A dimeric form of the enzyme would be expected, ab initio, to retain the catalytic and regulatory activity of the tetramer. However, we have recently engineered dimeric forms of *E. coli* DHDPS by in vitro mutagenesis, and have demonstrated that the dimer, although sharing an identical tertiary structure, possesses a significantly lower activity relative to the wild-type enzyme (Griffin et al., unpublished work). This indicates that tetramerisation is essential for function and that disruption of the tetrameric state may offer a novel means of enzyme inhibition.

GDP-mannose pyrophosphorylase

We have recently reported the self-association of GDP-MP, which forms a stable hexamer under physiological conditions (Davis et al. 2004b). Similar to DHDPS, the oligomeric species of GDP-MP represents the active form of the enzyme, whilst the monomer demonstrates no catalytic activity in vitro (Davis et al., unpublished). The GDP-MP plays a critical role in mannose metabolism in *Leishmania* species, where it is responsible for catalyzing the conversion of mannose-1-phosphate to GDP-mannose using GTP as the nucleoside-diphosphate donor (Davis et al. 2004b). The GDP-mannose is subsequently used as a building block for the production of glycoconjugate molecules. These glycoconjugates, including GPI-anchored lipids, are found on the outer glycocalyx of the parasite and are demonstrated to be important virulence factors in leishmaniasis (Handman 1992). This disease is estimated to infect over 12 million people worldwide and is largely endemic throughout tropical and sub-tropical regions, including northern Africa, southern Europe and South America (Handman 2001). To date, there is no vaccine against leishmaniasis and chemotherapy is still the only means of disease control (Handman 2001). The current drugs, based primarily on antimonial salts first introduced in the 1930s, are difficult to administer, are toxic, and drug resistance is increasing rapidly (Davis et al. 2004a). Accordingly, there is an urgent need for the development of new drugs, and therefore an urgent need to characterise novel drug targets. One such target is GDP-MP, and disruption of its oligomeric state would provide a novel means of inhibiting this important enzyme.

Experimental

Expression and purification of DHDPS

This was carried out according to previously-published methods (Dobson et al. 2004).

Analytical ultracentrifugation

Sedimentation experiments were performed in a Beckman Model XL-A analytical ultracentrifuge equipped with UV/Vis scanning optics and An-60 Ti 4-hole rotor at 20 °C. Protein sample (0.05–1.0 mg/ml) and reference (20 mM Tris–HCl, 150 mM NaCl, pH 8.0) solutions were loaded into 12 mm double sector cells with quartz windows. Prior to sedimentation, the protein samples were purified to homogeneity by size-exclusion liquid chromatography on a 16 × 600 mm Sephacryl S400 column (Pharmacia). For sedimentation velocity experiments, 380 µl of sample and 400 µl of reference were centrifuged at 40,000 rpm and data was collected at 230 or 280 nm every 6 min without averaging. For sedimentation equilibrium experiments, 100 µl of sample and 120 µl of reference were centrifuged at 10,000 or 16,000 rpm until sedimentation equilibrium was attained (24–36 h) and radial absorbance scans were taken at 230, 235 or 280 nm with ten averages. High-speed depletion was then performed at 40,000 rpm for up to 5 h and the baseline offset (E) was determined by averaging the absorbance over a 0.1 cm radial range in the solution plateau near the sample meniscus. The value of E in all cases, including sedimentation velocity experiments, represented $< 5\%$ of the total initial absorbance and was employed as a fixed parameter in the non-linear analyses described below. The partial specific volume $\bar{v}$ of the sample and the density and viscosity of the buffer were computed using the program SEDNTERP (Laue et al. 1992). Sedimentation velocity data was fitted to a single discrete species, multiple discrete species or a continuous size-distribution model using the program SEDFIT (Schuck 2000). Sedimentation equilibrium data were fitted globally at multiple speeds and wavelengths with and without sedimentation velocity data to a single discrete species, multiple discrete species or self-associating models using the program SEDPHAT (Vistica et al. 2004). The SEDFIT and SEDPHAT programs are available from http://www.analyticalultracentrifugation.com.

Molecular modeling

The MODELLER (6v2) package (Sali and Blundell 1993) was used to generate models of trimeric GDP-MP based on the sequence alignment generated by FUGUE (Shi et al. 2001) with *N*-acetyl-glucosamine-1-phosphate uridyltransferase (Glmu) from *Streptococcus pneumoniae* (Sulzenbacher et al. 2001), and glucose-1-phosphate thymidylyltransferase (RmlA) from *Pseudomonas aeruginosa* (Blankenfeldt et al. 2000). Initially, 25 models were generated and the model with lowest MODELLER objective function was used for further model building. Assessment of this model using Profiles-3D (Luthy et al. 1992) analysis indicated good amino acid environment compatibility. The FTDock (Gabb et al. 1997) program was used to generate hexameric models of GDP-MP by docking two trimeric GDP-MPs with a grid span of 0.8 Å, a surface thickness of 1.2 Å, and angle step of 12° applied to construct a total of 4000 hexameric models. These were then ranked according to an empirical pair

potential (Moont et al. 1999). Refinement of the interfaces was performed using the MULTIDOCK program (Jackson et al. 1998). Buried surface areas were calculated as the difference in solvent accessible surface areas in uncomplexed and complexed structures using the program NACCESS Version 2.1.1 (Hubbard and Thornton 1993).

Results and discussion

Techniques for measuring protein self-association

A number of techniques have been employed to measure self-association and hetero-association of proteins. Qualitatively, the common methods are analytical gel permeation liquid chromatography (Andrews 1964) and blue native PAGE (Schagger et al. 1994). These techniques are relatively simple and inexpensive, but can lead to aberrant results when analysing asymmetric macromolecules and rapidly diffusing or dissociating systems. Quantitatively, analytical ultracentrifugation is a superior method for measuring self-association or hetero-association (Perugini et al. 2000, 2002; Schuck et al. 2002). Despite the fact that the technique was first pioneered by Svedberg in the 1920s (van Holde and Hansen 1998), the major bottleneck of analytical ultracentrifugation for almost 80 years up to the turn of the millennium has been data analysis. The speed of the modern day computer now makes it possible to perform a billion iterations in a few seconds and so one can solve complicated algorithms in little time, including the Lamm equation, which describes the rate of movement of a macromolecule in a gravitational field (Schuck 2000). The development of continuous size-distribution [$c(s)$] analysis using the program SEDFIT (Schuck 2000) has provided an efficient approach to generating size-distribution profiles of heterogeneous macromolecular systems (Davis et al. 2004b; Perugini et al. 2000, 2002; Schuck et al. 2002). When compared to more traditional size-distribution analysis tools, including the van Holde–Weischet method and the $g^*(s)$ method, the $c(s)$ algorithm is superior in terms of sensitivity and resolution (Schuck et al. 2002). Accordingly, the identity of multiple species in the analytical ultracentrifuge can now be determined from a simple sedimentation velocity experiment without the need for time-laborious sedimentation equilibrium data (Perugini et al. 2000; Schuck et al. 2002). However, this analysis is restricted to non-interacting or slow equilibrium systems (Perugini et al. 2000; Schuck 2000). For characterisation of self-associating or hetero-associating systems, the recent development of the program SEDPHAT (Vistica et al. 2004) has enabled efficient global analyses to be performed with sedimentation equilibrium data with and without sedimentation velocity data sets. This approach has recently been successful in determining the hexamerisation of GDP-MP (Davis et al. 2004b) and is demonstrated below for the characterisation of the oligomeric structure of DHDPS.

Tetramerisation of DHDPS

To characterise the quaternary structure of DHDPS in aqueous solution, sedimentation velocity studies were

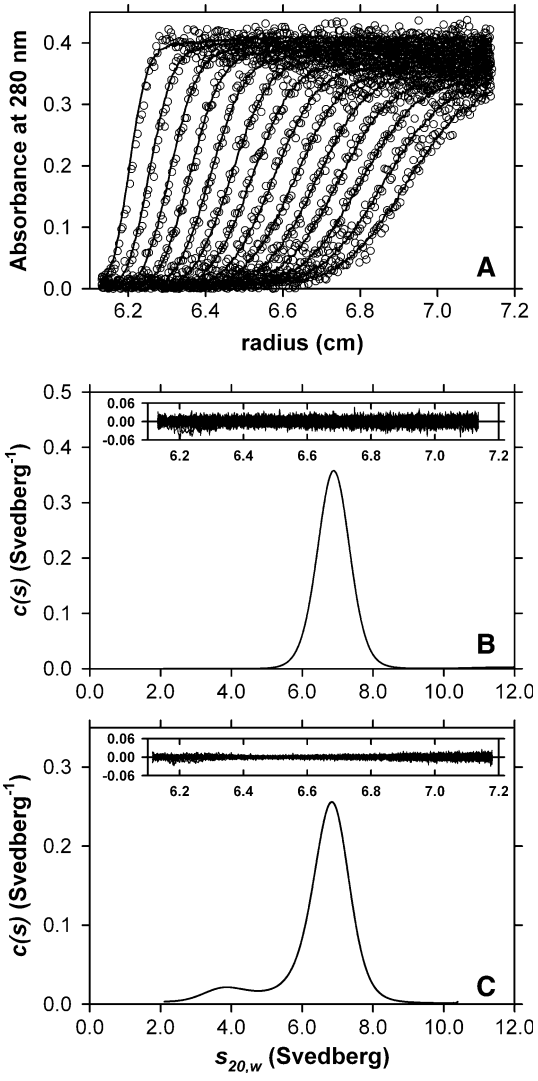

Fig. 2A–C Sedimentation velocity analyses of DHDPS. **A** Absorbance at 280 nm plotted as a function of radial position (cm) from axis of rotation for DHDPS at an initial concentration of 1.0 mg/ml. Raw data (*open symbols*) are plotted at time intervals of 12 min and are overlaid with the continuous size-distribution best-fit (*solid lines*) shown in **B**. **B** Continuous sedimentation coefficient [$c(s)$] plotted as a function of standardised sedimentation coefficient ($s_{20,w}$) for DHDPS at an initial protein concentration of 1.0 mg/ml. The RMSD and runs test Z values for the $c(s)$ distribution best fit shown were calculated to be 0.011 and 4.6, respectively. *Inset* Residuals plotted as a function of radial position (cm) from the axis of rotation. **C** $c(s)$ distribution plotted as a function of $s_{20,w}$ for DHDPS at an initial protein concentration of 50 μg/ml. The RMSD and runs test Z-value values for the $c(s)$ distribution best fit shown were calculated to be 0.0047 and 13, respectively. *Inset* Residuals plotted as a function of radial position (cm) from the axis of rotation. Continuous size-distribution analysis was performed using the program SEDFIT (Schuck 2000) at a resolution of 200 sedimentation coefficients between 0.5 and 12.5 S, with rotor speed ramping, at $P = 0.95$ and $f/f_0 = 1.25$ (**B**) and $f/f_0 = 1.62$ (**C**)

Table 1 Summary of the hydrodynamic properties of wild-type DHDPS

Oligomer	$s_{20,w}$[a] (S)	M_r[b] (kDa)	M[c] (kDa)	a/b[d]	K_D[e] (nM)	k_{off}[f] (s^{-1})
Dimer	3.9	62.5	69.8	4.5	–	–
Tetramer	6.9	125	128	2.6	76	3.2×10^{-5}

[a] Standardised sedimentation coefficient taken from the ordinate maximum of the $c(s)$ distribution best-fit (Figs. 2B and C)
[b] Relative molecular weight calculated from the amino acid sequence
[c] Apparent molar mass taken from the ordinate maximum of the $c(M)$ distribution best-fit (data not shown)
[d] Axial ratio assuming a prolate ellipsoid shape calculated using the $\bar{v}$ method (Laue et al. 1992)
[e] Tetramer dissociation constant, calculated from a global non-linear least squares best-fit to a dimer–tetramer equilibrium (Fig. 3)
[f] Rate constant for the dissociation of tetramer to dimer, calculated from the global non-linear least-squares best-fit described in Fig. 3

initially employed in the analytical ultracentrifuge. The data for DHDPS at an initial protein concentration of 1.0 mg/ml is plotted at 12 min intervals in Fig. 2A. These data were fitted to a continuous size-distribution model (Schuck 2000) yielding the $c(s)$ distribution shown in Fig. 2B, which indicates that DHDPS exists as a single species with a standardised sedimentation coefficient ($s_{20,w}$) of 6.9 S (Table 1). The molar mass of this species taken from the ordinate maximum of the $c(M)$ distribution is consistent with the mass of the DHDPS tetramer (Table 1). This suggests that DHDPS exists as a stable tetrameric species in aqueous solution at an initial protein concentration of 1.0 mg/ml, consistent with the crystal structure of the *E. coli* enzyme (Fig. 1), as well as gel permeation liquid chromatography and blue native PAGE studies described elsewhere (Griffin et al., unpublished work).

To determine whether the tetramerisation of DHDPS is concentration-dependent, particularly given the structure of the weak dimer–dimer interface (Fig. 1), sedimentation velocity experiments were also performed at an initial protein concentration of 0.05 mg/ml or 1.6 μM (Fig. 2C). The $c(s)$ distribution plotted in Fig. 2C shows that DHDPS exists as a mixture of two species with $s_{20,w}$ values of 3.9S and 6.9S that are not baseline-resolved (Fig. 2C, Table 1). Similar data was obtained using the $g^*(s)$ method (data not shown). This suggests that the enzyme resides in an equilibrium mixture of dimers and tetramers. Assuming a prolate ellipsoidal shape, the axial ratio for the dimer and tetramer are calculated to be 4.5 and 2.6, respectively, indicating that the dimeric species is more asymmetric in shape (Table 1). This may be due to increased flexibility in the dimer, as seen with dimeric mutants of DHDPS described elsewhere (Griffin et al., unpublished work). To confirm the state of association of the wild-type enzyme at low protein concentrations, and to quantitate the tetramerisation constant, sedimentation equilibrium experiments were subsequently performed at two rotor speeds, multiple wavelengths and varying initial protein concentrations of 0.05 and 0.3 mg/ml. These data were fitted globally with sedimentation velocity data obtained at an initial enzyme concentration of 0.05 mg/ml (Fig. 3A). The global non-linear least-squares best-fit yielded a tetramerisation constant ($K_{2,4}$) of 1.32×10^7 M^{-1} ($K_D = 76$ nM) and a rate constant for the dissociation of tetramer (k_{off}) of approximately 3.2×10^{-5} s^{-1} (Fig. 3, Table 1). This indicates that DHDPS exists in a slow dimer–tetramer equilibrium. By comparison, poor fits were obtained to a rapid ($k_{off} = 0.1$ s^{-1}) dimer–tetramer model (data not shown). Furthermore, poor fits were also calculated when the data shown in Fig. 3 were fitted to monomer–tetramer, monomer–trimer or dimer–hexamer equilibria (data not shown).

Hexamerisation and 3-D model of GDP-MP

Given the importance of GDP-MP as a novel drug target for leishmaniasis, there is considerable interest in determining the three-dimensional structure of GDP-MP. Previously we have shown in the analytical ultracentrifuge that GDP-MP self-associates as a dimer of trimers to form an asymmetric hexamer that is stable under physiological conditions (Davis et al. 2004b). Nevertheless, these studies do not provide insight into how the hexamer assembles. In particular, we are interested in elucidating whether the trimeric form of the enzyme associates to form a hexamer in a head-to-head (N-terminal to N-terminal) or tail-to-tail (C-terminal to C-terminal) manner. Both models are feasible based on the hydrodynamic shape calculated from sedimentation velocity studies (Davis et al. 2004b). Three-dimensional modeling of the enzyme was therefore performed.

Comparative sequence analysis suggests that GDP-MP from *L. mexicana* consists of two domains: an N-terminal nucleoside triphosphate (NTP) transferase domain and a C-terminal left-handed β-helix (LβH) domain (Fig. 4A). Its most closely related homologues in the PDB are Glmu, a uridyltransferase enzyme from *Steptococcus pneumoniae*, and RmlA, a thymidylyltransferase from *Pseudomonas aeruginosa*. A model of trimeric GDP-MP was therefore generated using the MODELLER program based on the known three-dimensional structures of Glmu (Sulzenbacher et al. 2001) and RmlA (Blankenfeldt et al. 2000) (PDB accession codes 1hm9 and 1fxo, respectively). The core subdomain (residues 1–245) of RmlA and the N-terminal domain of Glmu (residues 1–245), which adopt identical folds, were used as the templates for the N-terminal domain of GDP-MP. The LβH domain of

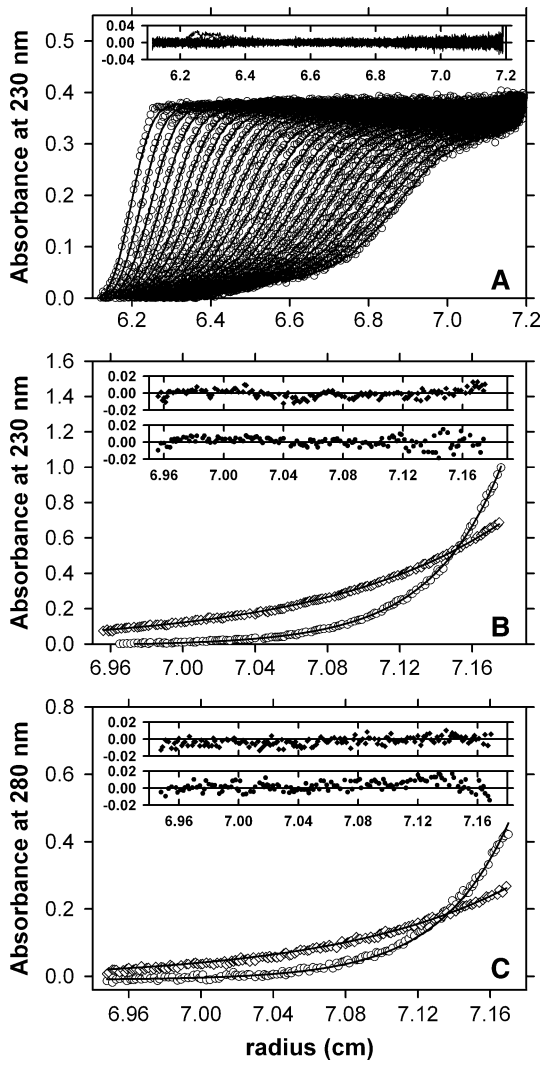

Fig. 3A–C Global dimer–tetramer self-association analysis of DHDPS sedimentation data. **A** Absorbance at 230 nm plotted as a function of radial position (cm) for DHDPS at an initial protein concentration of 0.05 mg/ml. Sedimentation velocity data (*open symbols*) are plotted at time intervals of 6 min and overlaid with the non-linear least-squares best-fit (*solid lines*) to a dimer–tetramer self-association model yielding $K_{2,4} = 1.3 \times 10^7$ M^{-1} ($K_D = 76$ nM) and $k_{off} = 3.2 \times 10^{-5}$ s^{-1}. *Inset* Residuals plotted as a function of radial position (cm) from the axis of rotation. The RMSD and runs test Z values were calculated as 0.0051 and 22, respectively. **B** Sedimentation equilibrium absorbance data at a wavelength of 230 nm for DHDPS at an initial protein concentration of 0.05 mg/ml at 10,000 rpm (*diamonds*) and 16,000 rpm (*circles*). The global non-linear least-square best-fit to a dimer–tetramer self-association model yielding parameters described in **A** above is represented by a *solid line*. *Insets* Residuals plotted as a function of radial position (cm)—10,000 rpm (*solid diamonds*) and 16,000 rpm (*solid circles*). The RMSD and runs test Z values were calculated as 0.0054 and 8.1, respectively. **C** Sedimentation equilibrium absorbance data at a wavelength of 280 nm for DHDPS at an initial protein concentration of 0.3 mg/ml at 10,000 rpm (*diamonds*) and 16,000 rpm (*circles*). Global non-linear least-square best-fit to the dimer–tetramer self-association model described above is represented by a *solid line*. *Insets* Residuals plotted as a function of radial position (cm)—10,000 rpm (*solid diamonds*) and 16,000 rpm (*solid circles*). The RMSD and runs test Z values were calculated as 0.0074 and 4.8, respectively

Glmu was used as a template for the C-terminal domain of GDP-MP. In Glmu, this domain packs tightly against the LβH domain of two other Glmu monomers to form a trimeric assembly. The LβH domain of Glmu consists of approximately 200 residues, constituting ten coils, with the final four coils forming the acetyl CoA binding site of enzyme. In comparison, the C-terminal domain of GDP-MP consists of approximately 120 residues forming six coils, and thus lacks the acyltransferase activity that Glmu possesses. A trimeric model of GDP-MP was constructed using the Glmu trimer as a template. Analysis of this model using Profiles-3D (Luthy et al. 1992) showed that most residues had a positive compatibility score, indicating favourable geometry. The total compatibility score of 386 for this structure compared favourably with the expected value for a protein of this size of 527 (Eisenberg et al. 1997).

Docked conformations of two GDP-MP trimers, forming hexamers, were calculated using the 3D-Dock suite of programs. Pair potentials were used to score the interactions across the interface of each hexameric complex (Moont et al. 1999), and the top 100 ranked models were then subjected to refinement using the program MULTIDOCK (Jackson et al. 1998). The structure with the highest rank after refinement is presented in Fig. 4B. In this structure, the two trimeric assemblies contact each other in a head-to-head manner involving only the N-terminal domain in such a way as to retain threefold symmetry. The structure is composed of 30% β strand, 25% α-helix and 13% turn, as determined using the program DSSP (Kabsch and Sander 1983), which is consistent with circular dichroism spectroscopy studies previously reported (Davis et al. 2004b). The modelled structure is approximately 140 Å long × 85 Å wide, which agrees well with the asymmetric shape of the hexamer calculated from sedimentation studies (Davis et al. 2004b), and buries 1209 $Å^2$ of surface at the trimer–trimer interface (Fig. 4B). This interface is formed by the interaction between a single monomer in each of the trimers and is thus composed of three unconnected regions forming a large cavity in the middle of the structure. The next highest ranked interaction presents an identical hexameric complex. The top two structures were ranked initially 40 and 79 from the shape complementary screen in FTDock, and 89 and 71, respectively, using the pair potential score. Examination of the top ten ranking hexamers reveals that only the top two complexes are precluded from forming higher order oligomers, which is consistent with analytical ultracentrifugation data described earlier (Davis et al. 2004b). By contrast, the alternative tail-to-tail arrangement, in which C-terminal domains form the interface, was ranked 1811 based on shape complementarity, and near the bottom of the ranking using the pair potential score. This arrangement buries only 945 $Å^2$ of surface at the interface. Accordingly, the top ranking structural model of GDP-MP (Fig. 4B) suggests that the enzyme self-associates to form a head-to-head hexameric structure.

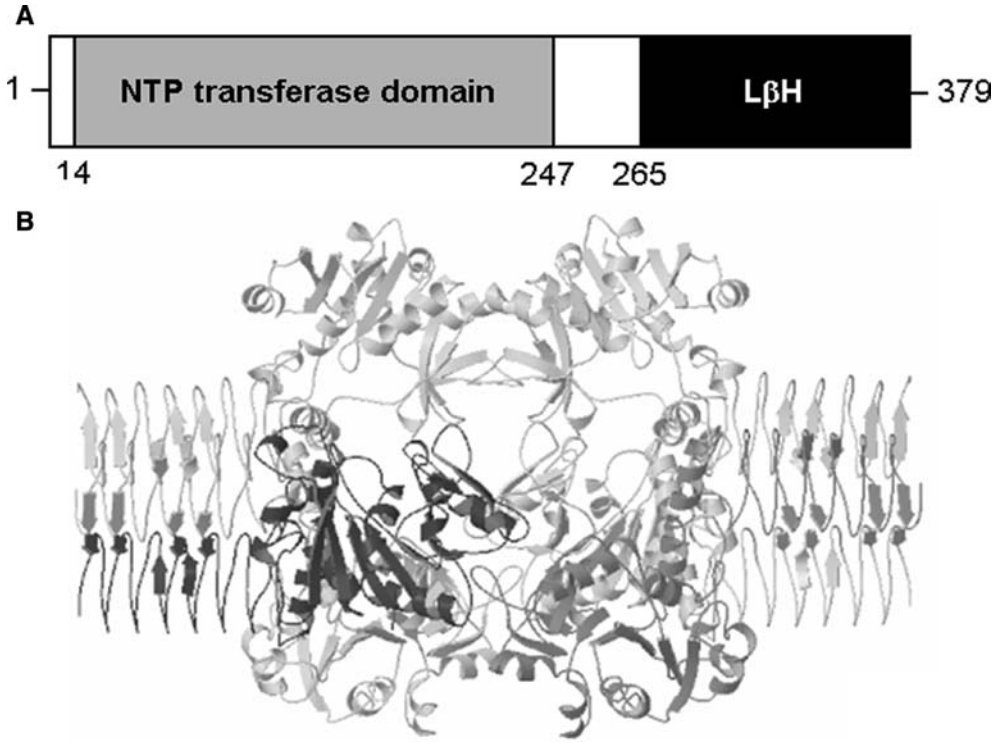

Fig. 4A–B Structure of GDP-MP from *Leishmania mexicana*. **A** Two-dimensional representation of the domain architecture of GDP-MP based on bioinformatics analyses using the Conserved Domain Database (CDD), which is available from http://www.ncbi.nlm.nih.gov/Structure/cdd/cdd.shtml. The N-terminal nucleoside triphosphate (*NTP*) transferase domain spans residues 14–247, whilst the C-terminal left-handed β-helix domain (LβH) is predicted to comprise of amino acids 265–379. **B** Three-dimensional model of the GDP-MP hexamer. The model reveals that the N-terminal domains of each trimer contact one another in a head-to-head manner that retains a threefold symmetry. To aid in visualizing how the hexamer is assembled, one monomer is represented in *light grey* and the other in *dark grey*. The dimensions of the hexamer shown are 140 Å long × 85 Å wide. The figure was generated using the programs MOLSCRIPT (Kraulis 1991) and Raster3D (Merritt and Bacon 1997)

This provides insight into the design of novel drugs that can inhibit the activity of this key enzyme in *Leishmania*.

Conclusions

In this study, we describe the structure of the DHDPS tetramer (Figs. 1, 2, 3) and a model of the GDP-MP hexamer (Fig. 4B). These structural analyses provide insight into the design of agents that can bind to and disrupt the oligomerisation interfaces of these enzymes. Disruption of protein interfaces in HIV-1 protease and triose phosphate isomerase has already been shown to provide new lead compounds in drug development. We propose that peptidomimetics or monoclonal antibodies can be generated to target the oligomerisation interfaces of key self-associating enzymes and thus be used as therapeutic agents for the treatment of infectious diseases, such as leishmaniasis. We foresee huge potential for drug development in this area and for the use of analytical ultracentrifugation as an essential tool in assessing the efficacy of this emerging class of therapeutics. Many drug targets, including DHDPS and GDP-MP, may be inhibited using this general paradigm.

Acknowledgements We thank Dr Michael Morris (University of Adelaide) for useful discussions surrounding the potential of disrupting the interface of DHDPS in the context of this paper and Prof Boris Martinac (University of Western Australia) for his encouragement and support during the preparation of this manuscript.

References

Andrews P (1964) Estimation of the molecular weights of proteins by sephadex gel-filtration. Biochem J 91:222–233

Blankenfeldt W, Asuncion M, Lam JS, Naismith JH (2000) The structural basis of the catalytic mechanism and regulation of glucose-1-phosphate thymidylyltransferase (RmlA). EMBO J 19:6652–6663

Boggetto N, Reboud-Ravaux M (2002) Dimerization inhibitors of HIV-1 protease. Biol Chem 383:1321–1324

Davis AJ, Murray HW, Handman E (2004a) Drugs against leishmaniasis: a synergy of technology and partnerships. Trends Parasitol 20:73–76

Davis AJ, Perugini MA, Smith BJ, Stewart JD, Ilg T, Hodder AN, Handman E (2004b) Properties of GDP-mannose pyrophosphorylase, a critical enzyme and drug target in *Leishmania mexicana*. J Biol Chem 279:12462–12468

Dobson RCD, Valegard K, Gerrard JA (2004) The crystal structure of three site-directed mutants of *Escherichia coli* dihydrodipicolinate synthase: further evidence for a catalytic triad. J Mol Biol 338:329–339

Eisenberg D, Luthy R, Bowie JU (1997) VERIFY3D: assessment of protein models with three-dimensional profiles. Methods Enzymol 277:396–404

Fenton AW, Paricharttanakul NM, Reinhart GD (2004) Disentangling the web of allosteric communication in a homotetramer: heterotropic activation in phosphofructokinase from *Escherichia coli*. Biochemistry 43:14104–14110

Gabb HA, Jackson RM, Sternberg MJ (1997) Modelling protein docking using shape complementarity, electrostatics and biochemical information. J Mol Biol 272:106–120

Handman E (1992) Host-parasite interactions in leishmaniasis. Adv Mol Cell Biol 5:133–155

Handman E (2001) Leishmaniasis: current status of vaccine development. Clin Microbiol Rev 14:229–243

van Holde KE, Hansen JC (1998) Analytical ultracentrifugation from 1924 to the present: a remarkable history. Chemtracts Biochem Mol Biol 11:933–943

Hubbard SJ, Thornton JM (1993) NACCESS. Computer Program, Department of Biochemistry and Molecular Biology, University College London

Hutton CA, Southwood TJ, Turner JJ (2003) Inhibitors of lysine biosynthesis as antibacterial agents. Mini Rev Med Chem 3:115–127

Jackson RM, Gabb HA, Sternberg MJ (1998) Rapid refinement of protein interfaces incorporating solvation: application to the docking problem. J Mol Biol 276:265–285

Kabsch W, Sander C (1983) Dictionary of protein secondary structure: pattern recognition of hydrogen-bonded and geometrical features. Biopolymers 22:2577–2637

Kraulis P (1991) MOLSCRIPT: a program to produce both detailed and schematic plots of protein structures. J Appl Crystallog 24:946–950

Laue TM, Shah BD, Ridgeway TM, Pelletier SL (1992) Computer-aided interpretation of analytical sedimentation data for proteins. In: Analytical ultracentrifugation in biochemistry and polymer science. The Royal Society of Chemistry, Cambridge, pp 90–125

Luthy R, Bowie JU, Eisenberg D (1992) Assessment of protein models with three-dimensional profiles. Nature 356:83–85

Marianayagam NJ, Sunde M, Matthews JM (2004) The power of two: protein dimerization in biology. Trends Biochem Sci 29:618–625

Martz F, Wilczynska M, Kleczkowski LA (2002) Oligomerisation status, with the monomer as the active species, defines catalytic efficiency of UDP-glucose pyrophosphorylase. Biochem J 367:295–300

Merritt EA, Bacon DJ (1997) Raster3D: photorealistic molecular graphics. Methods Enzymol 277:505–524

Mirwaldt C, Korndorfer I, Huber R (1995) The crystal structure of dihydrodipicolinate synthase from *Escherichia coli* at 2.5 Å resolution. J Mol Biol 246:227–239

Moont G, Gabb HA, Sternberg MJ (1999) Use of pair potentials across protein interfaces in screening predicted docked complexes. Proteins 35:364–373

Nooren IMA, Thornton JM (2003) Diversity of protein–protein interaction. EMBO J 22:3486–3492

Perugini MA, Schuck P, Howlett GJ (2000) Self-association of human apolipoprotein E3 and E4 in the presence and absence of phospholipid. J Biol Chem 275:36758–36765

Perugini MA, Schuck P, Howlett GJ (2002) Differences in the binding capacity of human apolipoprotein E3 and E4 to size-fractionated lipid emulsions. Eur J Biochem 269:5939–5949

Sali A, Blundell TL (1993) Comparative protein modelling by satisfaction of spatial restraints. J Mol Biol 234:779–815

Schagger H, Cramer WA, von Jagow G (1994) Analysis of molecular masses and oligomeric states of protein complexes by blue native electrophoresis and isolation of membrane protein complexes by two-dimensional native electrophoresis. Anal Biochem 217:220–230

Schuck P (2000) Size-distribution analysis of macromolecules by sedimentation velocity ultracentrifugation and Lamm equation modeling. Biophys J 78:1606–1619

Schuck P, Perugini MA, Gonzales NR, Howlett GJ, Schubert D (2002) Size-distribution analysis of proteins by analytical ultracentrifugation: strategies and application to model systems. Biophys J 82:1096–1111

Shi J, Blundell TL, Mizuguchi K (2001) FUGUE: sequence-structure homology recognition using environment-specific substitution tables and structure-dependent gap penalties. J Mol Biol 310:243–257

Singh SK, Maithal K, Balaram H, Balaram P (2001) Synthetic peptides as inactivators of multimeric enzymes: inhibition of *Plasmodium falciparum* triosephosphate isomerase by interface peptides. FEBS Lett 501:19–23

Sulzenbacher G, Gal L, Peneff C, Fassy F, Bourne Y (2001) Crystal structure of *Streptococcus pneumoniae*N-acetylglucosamine-1-phosphate uridyltransferase bound to acetyl-coenzyme A reveals a novel active site architecture. J Biol Chem 276:11844–11851

Vistica J, Dam J, Balbo A, Yikilmaz E, Mariuzza RA, Rouault TA, Schuck P (2004) Sedimentation equilibrium analysis of protein interactions with global implicit mass conservation constraints and systematic noise decomposition. Anal Biochem 326:234–256

Yonetani T, Park S, Tsuneshige A, Imai K, Kanaori K (2002) Global allostery model of hemoglobin. Modulation of O2 affinity, cooperativity, and Bohr effect by heterotropic allosteric effectors. J Biol Chem 277:34508–34520